Atmos. Meas. Tech., 9, 5193–5201, 2016
www.atmos-meas-tech.net/9/5193/2016/
doi:10.5194/amt-9-5193-2016

Atmospheric Measurement Techniques
Open Access
EGU

Inverse modelling of NO_x emissions over eastern China: uncertainties due to chemical non-linearity

Dasa Gu[1,a], Yuhang Wang[1], Ran Yin[1], Yuzhong Zhang[1], and Charles Smeltzer[1]

[1]School of Earth and Atmospheric Sciences, Georgia Institute of Technology, Atlanta, GA, USA
[a]now at: Department of Earth System Science, University of California, Irvine, USA

Correspondence to: Yuhang Wang (ywang@eas.gatech.edu)

Received: 22 April 2016 – Published in Atmos. Meas. Tech. Discuss.: 2 May 2016
Revised: 4 October 2016 – Accepted: 13 October 2016 – Published: 24 October 2016

Abstract. Satellite observations of nitrogen dioxide (NO_2) have often been used to derive nitrogen oxides ($NO_x = NO + NO_2$) emissions. A widely used inversion method was developed by Martin et al. (2003). Refinements of this method were subsequently developed. In the context of this inversion method, we show that the local derivative (of a first-order Taylor expansion) is more appropriate than the "bulk ratio" (ratio of emission to column) used in the original formulation for polluted regions. Using the bulk ratio can lead to biases in regions of high NO_x emissions such as eastern China due to chemical non-linearity. Inverse modelling using the local derivative method is applied to both GOME-2 and OMI satellite measurements to estimate anthropogenic NO_x emissions over eastern China. Compared with the traditional method using bulk ratio, the local derivative method produces more consistent NO_x emission estimates between the inversion results using GOME-2 and OMI measurements. The results also show significant changes in the spatial distribution of NO_x emissions, especially over high emission regions of eastern China. We further discuss a potential pitfall of using the difference of two satellite measurements to derive NO_x emissions. Our analysis suggests that chemical non-linearity needs to be accounted for and that a careful bias analysis is required in order to use the satellite differential method in inverse modelling of NO_x emissions.

1 Introduction

Nitrogen oxides ($NO_x = NO + NO_2$) play an important role in tropospheric photochemistry of ozone and secondary aerosol formation. They are normally emitted from both anthropogenic (e.g. fossil fuel combustion) and natural sources (e.g. lightning, soil and wild fire). The rapid economic growth in East Asia has led to a significant increase of energy consumption, thereby increasing anthropogenic NO_x emissions, during last two decades (Boersma et al., 2008; Ghude et al., 2009; Gu et al., 2013; Ma et al., 2006; Mijling et al., 2013; Richter et al., 2005; Stavrakou et al., 2008; van der A et al., 2006; Zhang et al., 2007).

The traditional bottom-up emission inventory relies on detailed information about sources and emission factors and, therefore, can have large uncertainties, especially in countries such as China where the emission information is incomplete (Streets et al., 2003). In recent years, satellite measurements of nitrogen dioxide (NO_2) from multiple instruments, including Global Ozone Monitoring Experiment (GOME), Scanning Imaging Absorption Spectrometer for Atmospheric Chartography (SCIAMACHY), Ozone Monitoring Instrument (OMI) and GOME-2, have been widely used to derive top-down estimation of NO_x emissions as an alternative to the bottom-up emission inventory (Gu et al., 2014; Jaegle et al., 2005; Lamsal et al., 2011; Lin et al., 2010; Stavrakou et al., 2008; Zhang et al., 2012).

Inverse modelling of NO_x emissions, incorporating model simulations and satellite observations, can help reduce uncertainties in bottom-up inventories, especially in China (Lin et al., 2012; Mijling and van der A, 2012; Zhao and Wang, 2009). Martin et al. (2003) developed the first monthly inversion method by scaling the bottom-up emission inventory with top-down constraints from GOME NO_2 column measurements. Zhao and Wang (2009) improved the method by carrying out the emission inversion iteratively on a daily ba-

sis. Gu et al. (2014) further refined this method by including column NO_2 retrieval in inverse modelling, which removes the biases introduced by inconsistency between NO_2 profiles in the retrieval and inverse modelling. Lin et al. (2010) developed a method of inverse modelling using column NO_2 difference between GOME-2 and OMI.

In the emission inversion problem, the top-down emission is estimated by modifying the a priori emission with a term proportional to the difference between the simulated and observed column density, which can be expressed as follows:

$$E = E_a + \alpha \times (\Omega_s - \Omega_m), \quad (1)$$

where E is the top-down emission, E_a is the a priori emission used in model simulation, Ω_s is the satellite-observed column, Ω_m is the model-simulated column and α is the correction rate. In the original formulation by Martin et al. (2003) and all subsequent studies using this or some variants of this method (e.g. Jaegle et al., 2005), α is calculated as the ratio between the a priori emission and simulated column (referred to as the bulk ratio hereafter).

$$\alpha = E_a/\Omega_m \quad (2)$$

Note that this formulation has an implicit assumption that the emission is linearly proportional to the column density. However, previous studies of the emission and column trends suggested that the non-linearity between NO_x emission and tropospheric NO_2 column is non-trivial (Gu et al., 2013; Lamsal et al., 2011; Lu and Streets, 2012; Stavrakou et al., 2008). This non-linear relationship is mainly due to the non-linear photochemical feedbacks between NO_x and OH (the increase in NO_x promotes OH production and reduces its lifetime in the low-emission condition, but suppresses OH production and increases its lifetime in the high-emission condition). Figure 1 shows tropospheric NO_2 column densities as a function of surface emissions at GOME-2 and OMI overpass time over eastern China simulated in the Regional chEmical and trAnsport Model (REAM) (model details are given in Sect. 2.2). Clearly, tropospheric NO_2 column is not linearly proportional to NO_x emission, which was assumed in Eq. (2). Another illustration of this problem for inverse modelling over China can be found in Gu et al. (2013). The difference in the non-linearity in the ratio of emission to column NO_2 between GOME-2 and OMI overpass time reflects in part the difference in the relative importance between transport and chemistry at a different time of day.

In this study, we examine whether considering the non-linear ratio between NO_x emissions and NO_2 columns can improve the inverse modelling results and reduce the discrepancies in emission estimates using different satellite observations. Applying the Taylor expansion to Eq. (1), we define a local derivative in place of the bulk ratio (Eq. 2). We implement the local derivative of emission to column NO_2 ratio in the REAM model and examine its effects on the inverse modelling estimates of surface anthropogenic NO_x emissions with GOME-2 and OMI measurements over China in August 2007. The new inversion results are compared to those using the bulk ratio method and the satellite differential method (Lin et al., 2010) and the implications for NO_x inverse modelling are discussed.

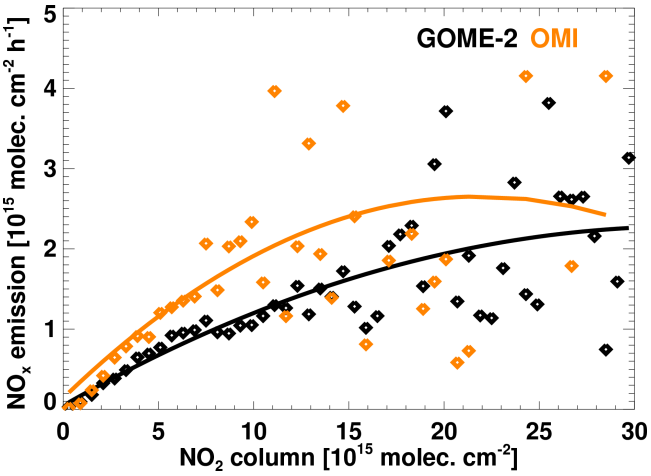

Figure 1. Simulated NO_2 column density as a function of surface NO_x emission at GOME-2 (black) and OMI (yellow) overpass time over eastern China for August 2007. The dots are grid average data from REAM simulations binned by a column NO_2 interval of 6×10^{14} mol cm^{-2} and the solid lines are from least-square polynomial regression results.

2 Satellite data and inverse modelling method

2.1 Satellite data

We use the measurements from GOME-2 and OMI instruments in this study. Both instruments are nadir-viewing spectrometers (Boersma et al., 2004, 2007, 2011). The OMI instrument was launched on board the Aura satellite in July 2004, and it has a spatial resolution of 24×13 km^2 at nadir (Levelt et al., 2006). The GOME-2 instrument used in this study was launched onboard the MetOp-A satellite in June 2006 with ground pixel size of 80×40 km^2 (Irie et al., 2012). The local overpass time across the equator is around 09:30 LT for GOME-2 and around 13:30 LT for OMI.

We use the Royal Netherlands Meteorological Institute (KNMI) OMI (DOMINO2 v2.0) and GOME-2 (TM4NO2A v2.3) tropospheric NO_2 vertical column density (VCD) products for this study. We excluded the data flagged with row anomalies from the OMI measurements (http://www.knmi.nl/omi/research/product/rowanomaly-background.php).
To reduce the cloud interference, we only use measured NO_2 column data when cloud fraction is <20 % for both measurements. The NO_2 VCD products were gridded to the REAM model domain with a 36×36 km^2 horizontal resolution.

The error in the retrieval of NO_2 tropospheric VCD is determined by those in total slant column density (SCD), stratospheric SCD and tropospheric air mass factor (AMF) estimation. In this study, we use total and stratospheric SCD errors from KNMI DOMINO2 and TM4NO2A products and compute the uncertainty of tropospheric AMF estimation following the KNMI algorithm. The details of error analysis were described by Boersma et al. (2004, 2007, 2011) and Hains et al. (2010). In general, the uncertainties of total and stratospheric SCD estimations are small ($< 0.7 \times 10^{15}$ mol cm^{-2}) relative to high tropospheric VCDs over eastern China (Zhao and Wang, 2009). The uncertainty in tropospheric AMF comes from surface albedo, cloud fraction, cloud pressure and profile shape. The uncertainty from an a priori profile can lead to ~ 10 % error in tropospheric VCD retrievals (Martin et al., 2003; Zhao and Wang, 2009). The total uncertainty of an individual retrieval is up to 50 % over highly polluted eastern China for both OMI and GOME-2. More detailed discussion of the retrieval uncertainties and their effects on NO_x emission inversion can be found in the studies by Boersma et al. (2004, 2007, 2011), Martin et al. (2003) and Zhao and Wang (2009).

2.2 REAM model

The 3-D REAM has been applied in a number of tropospheric chemistry and transport studies over East Asia, North America and polar regions (Choi et al., 2005, 2008a, b; Gu et al., 2013, 2014; Jing et al., 2006; Liu et al., 2010, 2012a, b; Wang et al., 2006, 2007; Yang et al., 2011; Zeng et al., 2003, 2006; Zhao et al., 2009a, b, 2010). The model has a horizontal resolution of 36×36 km^2 with 30 vertical layers in the troposphere. Transport is driven by WRF assimilated meteorological fields constrained by the NCEP reanalysis products (http://www.esrl.noaa.gov/psd/). The chemistry mechanism in the REAM is adopted from the GEOS-Chem model (Bey et al., 2001) with updates of kinetics data (http://jpldataeval.jpl.nasa.gov/). The anthropogenic NO_x and VOCs emissions are from Zhang et al. (2009). The biomass burning emissions are taken from the Global Fire Emissions Database, Version 2 (GFEDv2.1; available at http://daac.ornl.gov/). The algorithm of soil NO_x emissions follows Yienger and Levy (1995) as adopted by Wang et al. (1998). The lightning NO_x emission is parameterised as in Zhao et al. (2010). The simulation was conducted in August 2007 in this study. For consistence with both OMI and GOME-2 retrievals, the same model-simulated NO_2 VCDs on each day (at corresponding satellite overpass time) are collected with an averaging kernel for inverse modelling with both satellite products.

2.3 Inverse modelling method

In the bulk ratio inverse modelling, we use the same framework by Martin et al. (2003) outlined above. As discussed in the introduction, the bulk ratio (α) used in the traditional method is based on the assumption of a linear relationship between NO_x emission and tropospheric column NO_2, which is only accurate under a low emission condition. As shown in Fig. 1, using the bulk ratio for inverse modelling overlooks the non-linear chemical feedback of NO_x lifetime at different satellite overpass times, which not only affects the accuracy of inverse modelling results but also leads to inconsistencies between emission inversions using different satellite measurements. To account for the non-linearity, we apply the Taylor expansion to Eq. (1) and obtain a local derivative ratio (α^*) to replace Eq. (2):

$$\alpha^* = \Delta E_a / \Delta \Omega_{\mathrm{m}}, \tag{3}$$

where ΔE_a is the change of the a priori emission and $\Delta \Omega_{\mathrm{m}}$ is the change of model-simulated column.

The Taylor expansion formulation of Eqs. (1) and (3) is equivalent to the previous works by Vinken et al. (2014a, b) and Castellanos et al. (2014), who accounted for the non-linear chemistry effect by adding the ratio of relative emission to relative column NO_2 changes, first introduced by Lamsal et al. (2011), to the formulation of Eqs. (1) and (2). For inversion of ship emissions, Vinken et al. (2014b) computed averaged non-linear factors for selected regions with perturbations proportional to the model–observation column difference. For polluted regions, the effect of profile change is small (Zhang et al., 2016) and is not included in this study. In the previous studies, model sensitivities are computed with domain-wide emission perturbations. This approach introduces uncertainties since the column change in a given grid cell is affected by emission changes in both that grid cell and upwind grid cells; the effects of upwind grid cells are a complex function of emissions, chemistry and transport. As in Gu et al. (2013), we carried out single-cell-based emission perturbation in the 3-D REAM model to compute the value of α^*. We first archived the 3-D influxes of all model tracers at each time step in the standard simulation. In the perturbation simulation (15 % of anthropogenic NO_x emissions), the influxes of all model tracers for all grid cells were replaced with the archived values at each time step. Consequently, the emission perturbation only affects NO_x chemistry, out flux and concentration in the same grid cell. Using the perturbation and standard simulation results, we computed the value of α^* and applied it to Eq. (1) to estimate inverted NO_x emission over eastern China in August 2007 with GOME-2 and OMI observations. The results from the local derivative method are compared with those using the bulk ratio method in later sections.

The uncertainties of the a posteriori emissions come from those in a priori and top-down emission estimates (Martin et al., 2003). Uncertainties in top-down emission estimates are derived from those in tropospheric NO_2 VCD retrievals and model simulations. The retrieval uncertainty is discussed in Sect. 2.1. The uncertainty of model simulation is estimated at 30 % and that of the bottom-up inventory is ~ 60 % over China (Zhao and Wang, 2009). The overall uncertainty of

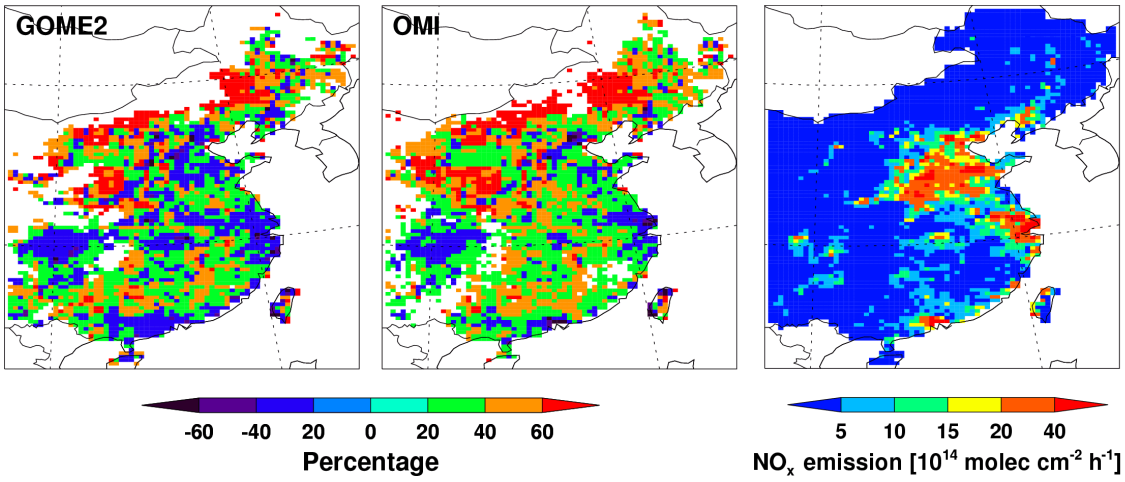

Figure 2. Relative difference between monthly mean local derivative ratio α^* and bulk ratio α, defined as $1-\alpha/\alpha^*$, for GOME-2 (left) and OMI (middle) in REAM simulations. The right panel shows NO_x emission distribution estimated from GOME-2 observations by using the local derivative method over eastern China for August 2007.

the a posteriori emission is typically in the range of 20–40 % over polluted eastern China (Gu et al., 2014; Zhao and Wang, 2009).

3 Results and discussion

3.1 Comparisons between α and α^*

Figure 2 compares the relative difference between local derivative ratio (α^*) and bulk ratio (α) values over eastern China for August 2007, at GOME-2 and OMI overpass times respectively. For both satellites, α^* is higher (> 20 %) than α over most low-emission rural regions but lower ($-20\sim-60$ %) than α over most high-emission regions including eastern coastal areas and Sichuan province. For emission estimates, the inversion biases over high emission regions tend to be more important than rural regions. The high bias of α relative to α^* implies that top-down NO_x emission estimates tend to over-correct for a given difference between observed and simulated column NO_2. We note here that the inversion bias can be either positive or negative depending on the column difference.

3.2 NO_x emission inversion consistency between OMI and GOME-2

Another way to look at the effects of correction biases using the bulk ratio relative to local derivative method is to compare the inversion estimated NO_x emissions using OMI and GOME-2 measurements. Gu et al. (2014) showed that inversion results using standard DOMINO products of GOME-2 tend to be higher than OMI possibly due to a bias in the TM4 NO_2 profiles used in GOME-2 retrievals. Coupling this tendency of a high retrieval bias of GOME-2 with the different sensitivities discussed in the previous paragraph implies that the bulk ratio formulation would tends to overcorrect and estimate higher NO_x emissions using GOME-2 than OMI measurements in polluted regions.

The bias expectation is confirmed in Fig. 3. While the inversion results using DOMINO GOME-2 and OMI products generally show higher NO_x emissions in the former, the difference between the inversions using two satellites is smaller using the local derivative than bulk ratio method, particularly over high emission regions. For example, we compare the emission estimates between the bulk ratio and local derivative methods in three largest megacities in China (e.g. Beijing, Shanghai and Guangzhou). Using the bulk ratio method, the relative difference of inversion emission estimates of using two satellites products relative to OMI results are 54.2, 70.5 and 55.6 % for the three megacities. The local derivative method reduces the corresponding relative differences down to 9.0, 5.3 and 13.5 % (Fig. 3 and Table 1). These results demonstrate that a significant fraction of the discrepancy in inverted NO_x emissions between different instruments can be attributed to neglecting the chemical non-linearity in the traditional bulk ratio method and that improvement can be achieved with the local derivative method that we proposed in this study. The remaining discrepancy between inversion emission estimates using GOME-2 and OMI observations is likely due to NO_2 profiles used in the retrieval and possible systematic biases between the two satellite instruments (Gu et al., 2014).

3.3 Comparison of inversion results between using the bulk ratio method and the satellite differential approach

Inversion can be applied to the column NO_2 measurements from two satellites (Lin and McElroy, 2010). Lin et al. (2010)

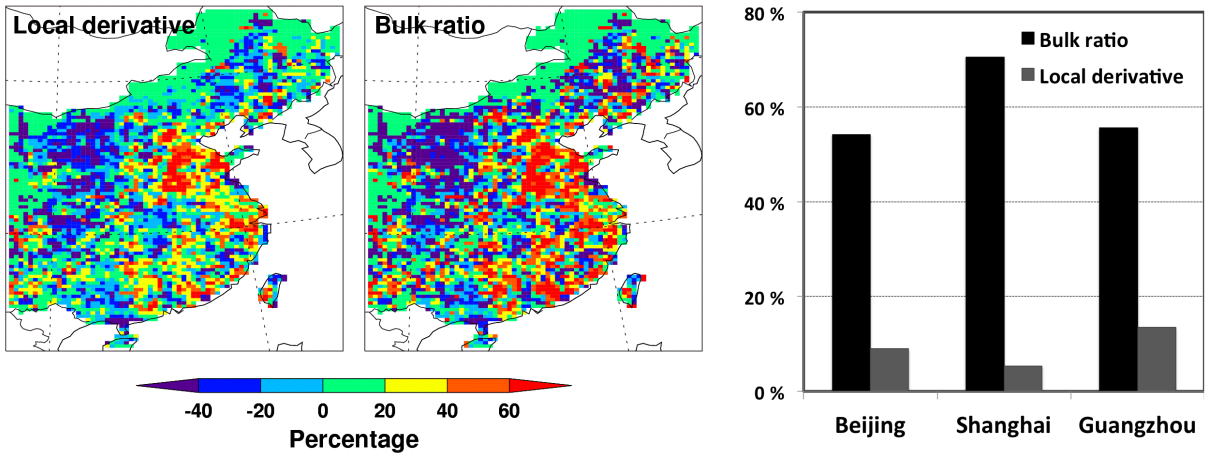

Figure 3. Relative difference of inversion emission estimates for NO_x with GOME-2 relative to OMI products using the local derivative and the bulk ratio methods: regional distributions over eastern China for August 2007 (left) and the differences in three megacities (right).

Table 1. NO_x inversion emission estimates for August 2007 using the local derivative, bulk ratio and satellite differential inversion methods.

Method		Emission rate (10^{15} mol cm^{-2} h^{-1}) Beijing	Shanghai	Guangzhou	Total Emission of Eastern China (Tg N yr^{-1})
Local derivative	GOME-2	7.78	13.8	4.71	6.18
	OMI	7.14	13.1	4.15	5.82
Bulk ratio	GOME-2	6.86	12.62	8.68	6.13
	OMI	4.45	7.40	5.58	5.50
Satellite differential		3.31	7.19	4.32	5.26
A priori estimates		9.68	16.9	4.76	5.27

developed a method to utilise information from two different satellites (referred to as the satellite differential method in this study) to improve the emission estimates. The formulation of the method can be simplified as follows,

$$\frac{E_j}{E_a} = \frac{\Omega_{\text{OMI}} - \Omega_{\text{GOME-2}} \cdot \exp(-t/\tau)}{\Omega_{\text{m1330}} - \Omega_{\text{m0930}} \cdot \exp(-t/\tau)}, \quad (4)$$

where E_j is the a posteriori emission, E_a is the a priori emission, Ω_{OMI} is OMI-observed NO_2 column, $\Omega_{\text{GOME-2}}$ is GOME-2-observed NO_2 column, Ω_{m1330} is model-simulated NO_2 column at OMI overpass time, Ω_{m0930} is model-simulated NO_2 column at GOME-2 overpass time, t is the time gap between two satellite overpass time and τ is the lifetime of NO_x. The derivation of this method is analogous to the bulk ratio method (Lin et al., 2010) and is not directly comparable to the local derivative method. We, therefore, compare the inversion results using the satellite differential method with those using the bulk ratio method.

In Table 1, the inversion emission estimates using the satellite differential method are compared with those using the bulk ratio method over eastern China in August 2007. As discussed in the previous section, the bulk ratio method leads to consistently high emission estimates using GOME-2 products compared to using OMI over high emission ratios, e.g. 50–70 % in the three megacities. The estimates using the satellite differential method are even lower than the bulk ratio inversion estimates using OMI products. The reason is that in our analysis $\Omega_{\text{GOME-2}}/\Omega_{\text{m0930}}$ is consistently larger than $\Omega_{\text{OMI}}/\Omega_{\text{m1330}}$ over eastern China (Fig. 4). The mathematical analysis in Appendix A shows that, consequently, a posteriori emission estimates using the satellite differential method are consistently lower than those using the bulk ratio method with either GOME-2 or OMI products. Lin and McElroy (2010) also noticed that the original Lin et al. (2010) method can lead to systematic inversion biases as we demonstrated here. They corrected the biases by not using the inversion results if the retrieved Ω_{OMI} and $\Omega_{\text{GOME-2}}$ are greater than 120 % of the simulated corresponding values. When the differences between the two satellite products are not well characterised, we find that the local derivative

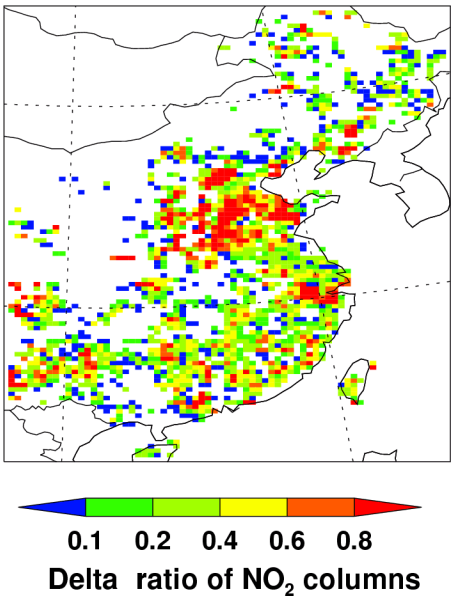

Figure 4. The distribution of $(\Omega_{\text{GOME-2}}/\Omega_{\text{m0930}}) - (\Omega_{\text{OMI}}/\Omega_{\text{m1330}})$ over eastern China for August 2007.

method is more robust relative to the bulk ratio and satellite differential methods (Table 1).

4 Conclusions

We show in this study that the non-linearity of NO_x chemistry implies that the local derivative (of a first-order Taylor expansion) is better suited in the inversion formulation developed by Martin et al. (2003) than bulk ratio, in agreement with Vinken et al. (2014a, b) and Castellanos et al. (2014). In this study, single-grid-cell-based perturbation sensitivity calculation was used instead of previous domain-wide perturbations such that upwind emission changes do not affect local derivative estimates. The latter effects can be more appropriately accounted for using the iterative method by Zhao and Wang (2009) and Gu et al. (2014). In the context of the inversion formulation by Martin et al. (2003), we compared the bulk ratio and local derivative methods in inverse modelling of anthropogenic NO_x emissions over eastern China for August 2007. At the observation time of OMI and GOME-2, the local derivative ratios (α^*) are smaller ($-20 \sim -60\,\%$) than the bulk ratios (α) over most high-emission regions, but are higher ($>20\,\%$) than bulk ratios (α) over most low-emission rural regions. Over high emission regions, the inversion emission estimates using the local derivative method produces more consistent results between OMI and GOME-2 products than the bulk ratio method. In our work, the observed to simulated tropospheric column NO_2 are consistently higher for GOME-2 than OMI over high emission regions of eastern China, leading to a consistent low bias in a posteriori emission estimates by the satellite differential method relative to those by the other methods. Computationally, the local derivative ratio is more complex to compute than bulk ratio. The iterative method in the previous work by Zhao and Wang (2009) and Gu et al. (2014) can largely mitigate the biases introduced by the bulk ratio method, although the inversion convergence time will likely be reduced when using local derivative than bulk ratios. For certain applications such as deriving the timeline of emission reduction during the Beijing Olympics (Yang et al., 2011), reducing the inversion convergence time is critically important. Further studies are needed to quantify the improvements.

5 Data availability

The KNMI OMI (DOMINO2 v2.0) and GOME-2 (TM4NO2A v2.3) tropospheric NO_2 VCD products used in this study are available at http://www.temis.nl/airpollution/no2.html. Other dataset are available on request to authors.

Appendix A

Table 1 shows that the inversion results using the satellite differential method are consistently lower than that of the bulk ratio method using OMI measurements, which are lower than the bulk ratio method using GOME-2 measurements over high emission regions. Lin and McElroy (2010) suggested it may be introduced by systematic errors in satellite retrievals. Here we show the mathematical analysis demonstrating the reasons for the consistent difference. In our analysis, the following inequality is found over high emission regions of eastern China (Fig. 4):

$$\frac{\Omega_{\text{GOME-2}}}{\Omega_{\text{m930}}} - \frac{\Omega_{\text{OMI}}}{\Omega_{\text{m1330}}} > 0. \tag{A1}$$

It follows that

$$\Omega_{\text{GOME-2}}\Omega_{\text{m1330}} - \Omega_{\text{OMI}}\Omega_{\text{m930}} > 0.$$

Therefore,

$$\Omega_{\text{OMI}}\Omega_{\text{m1330}} - \Omega_{\text{OMI}}\Omega_{\text{m930}}\exp(-\frac{t}{\tau}) > \Omega_{\text{OMI}}\Omega_{\text{m1330}} - \Omega_{\text{GOME-2}}\Omega_{\text{m1330}}\exp\left(-\frac{t}{\tau}\right)$$

and

$$\frac{\Omega_{\text{OMI}}\Omega_{\text{m1330}} - \Omega_{\text{GOME-2}}\Omega_{\text{m1330}}\exp\left(-\frac{t}{\tau}\right)}{\Omega_{\text{OMI}}\Omega_{\text{m1330}} - \Omega_{\text{OMI}}\Omega_{\text{m930}}\exp(-\frac{t}{\tau})} < 1.$$

We obtain

$$\frac{\Omega_{\text{OMI}} - \Omega_{\text{GOME-2}}\exp\left(-\frac{t}{\tau}\right)}{\Omega_{\text{m1330}} - \Omega_{\text{m930}}\exp(-\frac{t}{\tau})} < \frac{\Omega_{\text{OMI}}}{\Omega_{\text{m1330}}} < \frac{\Omega_{\text{GOME-2}}}{\Omega_{\text{m930}}}. \tag{A2}$$

Given a priori emission estimation of Eqs. (2) and (4), Eq. (A2) implies that

$$E_j < E_{b,\text{OMI}} < E_{b,\text{GOME-2}}, \tag{A3}$$

where E_j is the inversion emission estimate by the satellite differential method, $E_{b,\text{OMI}}$ is the inversion emission estimate by the bulk ratio method using OMI measurements, and $E_{b,\text{GOME-2}}$ is the inversion emission estimate by the bulk ratio method using GOME-2 measurements.

Acknowledgements. This work was supported by the NSF Atmospheric Chemistry and NASA ACMAP Programs. We acknowledge the free use of OMI and GOME-2 data and products from www.temis.nl. We thank Folkert Boersma for his suggestions.

Edited by: F. Boersma
Reviewed by: two anonymous referees

References

Bey, I., Jacob, D. J., Yantosca, R. M., Logan, J. A., Field, B. D., Fiore, A. M., Li, Q. B., Liu, H. G. Y., Mickley, L. J., and Schultz, M. G.: Global modeling of tropospheric chemistry with assimilated meteorology: Model description and evaluation, J. Geophys. Res.-Atmos., 106, 23073–23095, 2001.

Boersma, K. F., Eskes, H. J., and Brinksma, E. J.: Error analysis for tropospheric NO_2 retrieval from space, J. Geophys. Res., 109, D04311, doi:10.1029/2003JD003962, 2004.

Boersma, K. F., Eskes, H. J., Veefkind, J. P., Brinksma, E. J., van der A, R. J., Sneep, M., van den Oord, G. H. J., Levelt, P. F., Stammes, P., Gleason, J. F., and Bucsela, E. J.: Near-real time retrieval of tropospheric NO_2 from OMI, Atmos. Chem. Phys., 7, 2103–2118, doi:10.5194/acp-7-2103-2007, 2007.

Boersma, K. F., Jacob, D. J., Eskes, H. J., Pinder, R. W., Wang, J., and van der A, R. J.: Intercomparison of SCIAMACHY and OMI tropospheric NO_2 columns: Observing the diurnal evolution of chemistry and emissions from space, J. Geophys. Res., 113, D16S26, doi:10.1029/2007JD008816, 2008.

Boersma, K. F., Eskes, H. J., Dirksen, R. J., van der A, R. J., Veefkind, J. P., Stammes, P., Huijnen, V., Kleipool, Q. L., Sneep, M., Claas, J., Leitão, J., Richter, A., Zhou, Y., and Brunner, D.: An improved tropospheric NO_2 column retrieval algorithm for the Ozone Monitoring Instrument, Atmos. Meas. Tech., 4, 1905–1928, doi:10.5194/amt-4-1905-2011, 2011.

Castellanos, P., Boersma, K. F., and van der Werf, G. R.: Satellite observations indicate substantial spatiotemporal variability in biomass burning NO_x emission factors for South America, Atmos. Chem. Phys., 14, 3929–3943, doi:10.5194/acp-14-3929-2014, 2014.

Choi, Y., Wang, Y. H., Zeng, T., Martin, R. V., Kurosu, T. P., and Chance, K.: Evidence of lightning NO_x and convective transport of pollutants in satellite observations over North America, Geophys. Res. Lett., 32, L02806, doi:10.1029/2004GL021436, 2005.

Choi, Y., Wang, Y., Zeng, T., Cunnold, D., Yang, E. S., Martin, R., Chance, K., Thouret, V., and Edgerton, E.: Springtime transitions of NO_2, CO, and O_3 over North America: Model evaluation and analysis, J. Geophys. Res.-Atmos., 113, D20311, doi:10.1029/2007JD009632, 2008a.

Choi, Y., Wang, Y. H., Yang, Q., Cunnold, D., Zeng, T., Shim, C., Luo, M., Eldering, A., Bucsela, E., and Gleason, J.: Spring to summer northward migration of high O_3 over the western North Atlantic, Geophys. Res. Lett., 35, L04802, doi:10.1029/2007GL032276, 2008b.

Ghude, S. D., Van der A, R. J., Beig, G., Fadnavis, S., and Polade, S. D.: Satellite derived trends in NO_2 over the major global hotspot regions during the past decade and their inter-comparison, Environ. Pollut., 157, 1873–1878, 2009.

Gu, D., Wang, Y., Smeltzer, C., and Liu, Z.: Reduction in NO_x Emission Trends over China: Regional and Seasonal Variations, Environ. Sci. Technol., 47, 12912–12919, 2013.

Gu, D., Wang, Y., Smeltzer, C., and Boersma, K. F.: Anthropogenic emissions of NO_x over China: Reconciling the difference of inverse modeling results using GOME-2 and OMI measurements, J. Geophys. Res.-Atmos., 119, JD021644, doi:10.1002/2014JD021644, 2014.

Hains, J. C., Boersma, K. F., Kroon, M., Dirksen, R. J., Cohen, R. C., Perring, A. E., Bucsela, E., Volten, H., Swart, D. P. J., Richter, A., Wittrock, F., Schoenhardt, A., Wagner, T., Ibrahim, O. W., van Roozendael, M., Pinardi, G., Gleason, J. F., Veefkind, J. P., and Levelt, P.: Testing and improving OMI DOMINO tropospheric NO_2 using observations from the DANDELIONS and INTEX-B validation campaigns, J. Geophys. Res.-Atmos., 115, D05301, doi:10.1029/2009JD012399, 2010.

Irie, H., Boersma, K. F., Kanaya, Y., Takashima, H., Pan, X., and Wang, Z. F.: Quantitative bias estimates for tropospheric NO_2 columns retrieved from SCIAMACHY, OMI, and GOME-2 using a common standard for East Asia, Atmos. Meas. Tech., 5, 2403–2411, doi:10.5194/amt-5-2403-2012, 2012.

Jaegle, L., Steinberger, L., Martin, R. V., and Chance, K.: Global partitioning of NO_x sources using satellite observations: Relative roles of fossil fuel combustion, biomass burning and soil emissions, Faraday Discuss., 130, 407–423, 2005.

Jing, P., Cunnold, D., Choi, Y., and Wang, Y.: Summertime tropospheric ozone columns from Aura OMI/MLS measurements versus regional model results over the United States, Geophys. Res. Lett., 33, L17817, doi:10.1029/2006GL026473, 2006.

Lamsal, L. N., Martin, R. V., Padmanabhan, A., van Donkelaar, A., Zhang, Q., Sioris, C. E., Chance, K., Kurosu, T. P., and Newchurch, M. J.: Application of satellite observations for timely updates to global anthropogenic NO_x emission inventories, Geophys. Res. Lett., 38, L05810, doi:10.1029/2010GL046476, 2011.

Levelt, P. F., Hilsenrath, E., Leppelmeier, G. W., van den Oord, G. H. J., Bhartia, P. K., Tamminen, J., de Haan, J. F., and Veefkind, J. P.: Science objectives of the Ozone Monitoring Instrument, IEEE Trans. Geosci. Remote, 44, 1199–1208, 2006.

Lin, J. T. and McElroy, M. B.: Impacts of boundary layer mixing on pollutant vertical profiles in the lower troposphere: Implications to satellite remote sensing, Atmos. Environ., 44, 1726–1739, 2010.

Lin, J. T., McElroy, M. B., and Boersma, K. F.: Constraint of anthropogenic NO_x emissions in China from different sectors: a new methodology using multiple satellite retrievals, Atmos. Chem. Phys., 10, 63–78, doi:10.5194/acp-10-63-2010, 2010.

Lin, J. T., Liu, Z., Zhang, Q., Liu, H., Mao, J., and Zhuang, G.: Modeling uncertainties for tropospheric nitrogen dioxide columns affecting satellite-based inverse modeling of nitrogen oxides emissions, Atmos. Chem. Phys., 12, 12255–12275, doi:10.5194/acp-12-12255-2012, 2012.

Liu, Z., Wang, Y. H., Gu, D. S., Zhao, C., Huey, L. G., Stickel, R., Liao, J., Shao, M., Zhu, T., Zeng, L. M., Liu, S. C., Chang, C. C., Amoroso, A., and Costabile, F.: Evidence of Reactive Aromatics As a Major Source of Peroxy Acetyl Nitrate over China, Environ. Sci. Technol., 44, 7017–7022, 2010.

Liu, Z., Wang, Y., Gu, D., Zhao, C., Huey, L. G., Stickel, R., Liao, J., Shao, M., Zhu, T., Zeng, L., Amoroso, A., Costabile,

F., Chang, C. C., and Liu, S. C.: Summertime photochemistry during CAREBeijing-2007: RO_x budgets and O_3 formation, Atmos. Chem. Phys., 12, 7737–7752, doi:10.5194/acp-12-7737-2012, 2012a.

Liu, Z., Wang, Y., Vrekoussis, M., Richter, A., Wittrock, F., Burrows, J. P., Shao, M., Chang, C.-C., Liu, S.-C., Wang, H., and Chen, C.: Exploring the missing source of glyoxal (CHOCHO) over China, Geophys. Res. Lett., 39, L10812, doi:10.1029/2012GL051645, 2012b.

Lu, Z. and Streets, D. G.: Increase in NO_x Emissions from Indian Thermal Power Plants during 1996–2010: Unit-Based Inventories and Multisatellite Observations, Environ. Sci. Technol., 46, 7463–7470, doi:10.1021/es300831w, 2012.

Ma, J. Z., Richter, A., Burrows, J. P., Nuss, H., and van Aardenne, J. A.: Comparison of model-simulated tropospheric NO_2 over China with GOME-satellite data, Atmos. Environ., 40, 593–604, 2006.

Martin, R. V., Jacob, D. J., Chance, K., Kurosu, T. P., Palmer, P. I., and Evans, M. J.: Global inventory of nitrogen oxide emissions constrained by space-based observations of NO_2 columns, J. Geophys. Res.-Atmos., 108, 4559, doi:10.1029/2003JD003453, 2003.

Mijling, B. and van der A, R. J.: Using daily satellite observations to estimate emissions of short-lived air pollutants on a mesoscopic scale, J. Geophys. Res., 117, D17302, doi:10.1029/2012JD017817, 2012.

Mijling, B., van der A, R. J., and Zhang, Q.: Regional nitrogen oxides emission trends in East Asia observed from space, Atmos. Chem. Phys., 13, 12003–12012, doi:10.5194/acp-13-12003-2013, 2013.

Richter, A., Burrows, J. P., Nuss, H., Granier, C., and Niemeier, U.: Increase in tropospheric nitrogen dioxide over China observed from space, Nature, 437, 129–132, 2005.

Stavrakou, T., Muller, J. F., Boersma, K. F., De Smedt, I., and van der A, R. J.: Assessing the distribution and growth rates of NO_x emission sources by inverting a 10-year record of NO_2 satellite columns, Geophys. Res. Lett., 35, L10803, doi:10.1029/2008GL033521, 2008.

Streets, D. G., Bond, T. C., Carmichael, G. R., Fernandes, S. D., Fu, Q., He, D., Klimont, Z., Nelson, S. M., Tsai, N. Y., Wang, M. Q., Woo, J. H., and Yarber, K. F.: An inventory of gaseous and primary aerosol emissions in Asia in the year 2000, J. Geophys. Res.-Atmos., 108, D218809, doi:10.1029/2002JD003093, 2003.

van der A, R. J., Peters, D., Eskes, H., Boersma, K. F., Van Roozendael, M., De Smedt, I., and Kelder, H. M.: Detection of the trend and seasonal variation in tropospheric NO_2 over China, J. Geophys. Res.-Atmos., 111, D12317, doi:10.1029/2005JD006594, 2006.

Vinken, G. C. M., Boersma, K. F., Maasakkers, J. D., Adon, M., and Martin, R. V.: Worldwide biogenic soil NO_x emissions inferred from OMI NO_2 observations, Atmos. Chem. Phys., 14, 10363–10381, doi:10.5194/acp-14-10363-2014, 2014a.

Vinken, G. C. M., Boersma, K. F., van Donkelaar, A., and Zhang, L.: Constraints on ship NO_x emissions in Europe using GEOS-Chem and OMI satellite NO_2 observations, Atmos. Chem. Phys., 14, 1353–1369, doi:10.5194/acp-14-1353-2014, 2014b.

Wang, Y., Jacob, D. J., and Logan, J. A.: Global simulation of tropospheric O_3-NO_x-hydrocarbon chemistry: 3. Origin of tropospheric ozone and effects of nonmethane hydrocarbons, J. Geophys. Res., 103, 10757–10767, 1998.

Wang, Y., Choi, Y., Zeng, T., Davis, D., Buhr, M., Huey, L. G., and Neff, W.: Assessing the photochemical impact of snow NO_x emissions over Antarctica during ANTCI 2003, Atmos. Environ., 41, 3944–3958, 2007.

Wang, Y. H., Choi, Y. S., Zeng, T., Ridley, B., Blake, N., Blake, D., and Flocke, F.: Late-spring increase of trans-Pacific pollution transport in the upper troposphere, Geophys. Res. Lett., 33, L01818, doi:10.1029/2005GL024975, 2006.

Yang, Q., Wang, Y., Zhao, C., Liu, Z., Gustafson, W. I., and Shao, M.: NO_x Emission Reduction and its Effects on Ozone during the 2008 Olympic Games, Environ. Sci. Technol., 45, 6404–6410, 2011.

Yienger, J. J. and Levy II, H.: Empirical model of global soil-biogenic NO_x emissions, J. Geophys. Res., 100, 11447–11464, 1995.

Zeng, T., Wang, Y., Chance, K., Blake, N., Blake, D., and Ridley, B.: Halogen-driven low-altitude O_3 and hydrocarbon losses in spring at northern high latitudes, J. Geophys. Res.-Atmos., 111, D17313, doi:10.1029/2005JD006706, 2006.

Zeng, T., Wang, Y. H., Chance, K., Browell, E. V., Ridley, B. A., and Atlas, E. L.: Widespread persistent near-surface ozone depletion at northern high latitudes in spring, Geophys. Res. Lett., 30, 8043, doi:10.1029/2003GL018587, 2003.

Zhang, Q., Streets, D. G., He, K., Wang, Y., Richter, A., Burrows, J. P., Uno, I., Jang, C. J., Chen, D., Yao, Z., and Lei, Y.: NO_x emission trends for China, 1995–2004: The view from the ground and the view from space, J. Geophys. Res.-Atmos., 112, D22204, doi:10.1029/2007JD008684, 2007.

Zhang, Q., Streets, D. G., Carmichael, G. R., He, K. B., Huo, H., Kannari, A., Klimont, Z., Park, I. S., Reddy, S., Fu, J. S., Chen, D., Duan, L., Lei, Y., Wang, L. T., and Yao, Z. L.: Asian emissions in 2006 for the NASA INTEX-B mission, Atmos. Chem. Phys., 9, 5131–5153, doi:10.5194/acp-9-5131-2009, 2009.

Zhang, Q., Geng, G. N., Wang, S. W., Richter, A., and He, K. B.: Satellite remote sensing of changes in NO_x emissions over China during 1996–2010, Chin. Sci. Bull., 57, 2857–2864, 2012.

Zhang, Y., Wang, Y., Chen, G., Smeltzer, C., Crawford, J., Olson, J., Szykman, J., Weinheimer, A. J., Knapp, D. J., Montzka, D. D., Wisthaler, A., Mikoviny, T., Fried, A., and Diskin, G.: Large vertical gradient of reactive nitrogen oxides in the boundary layer: Modeling analysis of DISCOVER-AQ 2011 observations, J. Geophys. Res.-Atmos., 121, 1922–1934, 2016.

Zhao, C. and Wang, Y.: Assimilated inversion of NOx emissions over east Asia using OMI NO_2 column measurements, Geophys. Res. Lett., 36, L06805, doi:10.1029/2008GL037123, 2009.

Zhao, C., Wang, Y., Choi, Y., and Zeng, T.: Summertime impact of convective transport and lightning NO_x production over North America: modeling dependence on meteorological simulations, Atmos. Chem. Phys., 9, 4315–4327, doi:10.5194/acp-9-4315-2009, 2009a.

Zhao, C., Wang, Y. H., and Zeng, T.: East China Plains: A "Basin" of Ozone Pollution, Environ. Sci. Technol., 43, 1911–1915, 2009b.

Zhao, C., Wang, Y., Yang, Q., Fu, R., Cunnold, D., and Choi, Y.: Impact of East Asian summer monsoon on the air quality over China: View from space, J. Geophys. Res.-Atmos., 115, D09301, doi:10.1029/2009JD012745, 2010.